

# Damage detection of shear buildings using frequency-change-ratio and model updating algorithm

Yabin Liang<sup>1,2</sup>, Qian Feng<sup>\*1,2</sup>, Heng Li<sup>1,2</sup> and Jian Jiang<sup>1,2</sup>

<sup>1</sup>Hubei Key Laboratory of Earthquake Early Warning, Institute of Seismology, CEA, Wuhan, China  
<sup>2</sup>Wuhan Institute of Earthquake Engineering Co Ltd, Wuhan, China

(Received March 6, 2018, Revised December 24, 2018, Accepted December 26, 2018)

**Abstract.** As one of the most important parameters in structural health monitoring, structural frequency has many advantages, such as convenient to be measured, high precision, and insensitive to noise. In addition, frequency-change-ratio based method had been validated to have the ability to identify the damage occurrence and location. However, building a precise enough finite elemental model (FEM) for the test structure is still a huge challenge for this frequency-change-ratio based damage detection technique. In order to overcome this disadvantage and extend the application for frequencies in structural health monitoring area, a novel method was developed in this paper by combining the cross-model cross-mode (CMCM) model updating algorithm with the frequency-change-ratio based method. At first, assuming the physical parameters, including the element mass and stiffness, of the test structure had been known with a certain value, then an initial to-be-updated model with these assumed parameters was constructed according to the typical mass and stiffness distribution characteristic of shear buildings. After that, this to-be-updated model was updated using CMCM algorithm by combining with the measured frequencies of the actual structure when no damage was introduced. Thus, this updated model was regarded as a representation of the FEM model of actual structure, because their modal information were almost the same. Finally, based on this updated model, the frequency-change-ratio based method can be further proceed to realize the damage detection and localization. In order to verify the effectiveness of the developed method, a four-level shear building was numerically simulated and two actual shear structures, including a three-level shear model and an eight-story frame, were experimentally test in laboratory, and all the test results demonstrate that the developed method can identify the structural damage occurrence and location effectively, even only very limited modal frequencies of the test structure were provided.

**Keywords:** cross-model cross-mode model updating algorithm; structural frequency-change-ratio based method; structural health monitoring; damage detection; shear buildings

## 1. Introduction

Due to its distinguish advantages, such as convenient to be measured, insensitive to disturbance, high measurement resolution and so on, structural frequency has been an attractive diagnostic parameter in structural assessment procedures, and has the potential to be applied in the practical application (Salawu 1997, Song *et al.* 2011, Li and He 2011). Therefore, many researchers have attempted to detect structural integrity through the changes in natural frequencies (Świder *et al.* 2012, Liu *et al.* 2015, Nagarajaiah and Yang 2015). However, since natural frequencies can only provide the global information of structures, it is difficult to obtain more detail information about the damage, such as the location and severity. In addition, the insensitive to small defect for structural frequency also limit its application in the area of structural health monitoring and damage diagnose.

On the other hand, by combining with other structural characteristic parameters and the related analysis

algorithms, some frequency-based methods had been developed to attempt to obtain more information about the structural integrity. For example, Xiang *et al.* (2009, 2011, 2012, 2014) presented a series of researches on the frequency-based method to detect the crack location and depth, especially for the beam-like structures, when combining with the mode shape curvature or other parameters. Ismail and Ong (2012) proposed a technique to determine the location and severity of honeycomb damage in a reinforced concrete beam using frequency mode shape regression focusing on minimal data. Unfortunately, compared to the modal frequency, there are still no other structural parameters that have the same advantages that can be conveniently obtained with the high precision, thus it is very meaningful to develop a frequency-only based method to take full advantage of the frequency to realize the structural damage detection.

In 1979, Cawley and Adams (1979) proposed a frequency-only based damage detection approach using the sensitivity concept, and this approach was based on the premise that the ratio of frequency changes in two modes is a function of the location of the damage only, if changes in stiffness are independent of frequency. To locate the defect, theoretical frequency shifts, due to damage at selected positions on the structure, are calculated and compared with

---

\*Corresponding author, Senior Engineer  
E-mail: [fengqian@eqhb.gov.cn](mailto:fengqian@eqhb.gov.cn)

measured values. In 1991, Hearn and Testa (1991) validated that frequency-change-square-ratio (FCSR), which is normalized with respect to the largest frequency change, is independent of severity for small deterioration and can be employed to indicate the location of deterioration directly. In 1994, based on theoretical derivation, Narkis (1994) proved that ratio of the frequency changes only associated with the damage location, but the physical dimension and property of the test structure. Then, Hassiots (1995) deduced the relationship between natural frequency changes and the changes of the stiffness matrix, and built the optimization model by employing the least square method, and then this model was successfully utilized to identify the damage location and severity of a 10-story steel frame structure and a cantilever beam just using the first five frequency-changes. Morassis and Rovere (1997) built an optimization model by utilizing the analysis frequencies and the measured frequencies of the structure, and a damage identification was successfully conducted by using the first five frequency-change ratio for a five-story steel framed structure.

For frequency-change-ratio based damage detection techniques, even only the measured frequencies of the test structure are provided, the structural integrity, including the damage occurrence and location, can be monitored and identified accurately. This distinguish advantage makes it potential to be widely applied especially in the adverse measurement environment of the actual structures. For these frequency-only based diagnose methods, calculating and extracting the theoretical frequency changes due to damage at selected position on the structure, is inevitable and essential, and directly influence the final identification results. However, it is always difficult, or even impossible for huge or complicate structure to obtain the theoretical modal parameters because of the huge uncertainty for the structural theoretical model. All this makes the frequency-change-ratio based technique still face a lot of challenges when be used in the structural health monitoring area for the practical applications.

In order to improve the feasibility of frequency-change-ratio based method in structural health monitoring, a novel approach was developed in this paper to help to realize the structure damage identification by combining the FCSR-based method with the cross-model cross-mode model updating algorithm. At the beginning, based on the typical mass and stiffness distribution characteristic of shear buildings, a model was initially assumed and constructed by the CMCM technique combining with the measured acceleration data of actual structure when no damage was introduced. Then, this model was utilized to represent the structural theoretical model to calculate and construct the FCSR-based baseline datasets. In addition, Model Assurance Criterion (MAC) and Normalized Modal Difference (NMD) methods were employed to quantify and evaluate the identification result. Finally, the structural health condition, especially the damage occurrence and location, can be identified accurately. In order to verify the effectiveness of the developed method, a four-level shear building was numerically simulated and two actual shear structures, including a three-level shear model and an eight-

story frame, were experimentally test in the laboratory. All the results demonstrate that the developed method can help to realize the structural damage diagnose when only the measured frequencies of the structure under health and test conditions are provided, and no structural theoretical model is needed.

## 2. Theoretical foundation

In order to clearly describe the developed method of this paper, the related basic theoretical foundations were first briefly introduced in this section, including the cross-model cross-mode model updating algorithm and the frequency-change-square-ratio based damage detection method. In addition, the MAC and NMD evaluation criterions were also mentioned here.

### 2.1 Cross-model cross-mode model updating algorithm

In 2007, Hu *et al.* (2007) developed a direct, physical property adjustment model updating method, named as cross-model cross-mode (CMCM) method, this new method is capable of updating the mass and stiffness matrices simultaneously based on very limited measured mode shapes and modal frequencies. Then, Wang (2009) successfully applied this technique to identify the structural health condition, both the theoretical deviation and numerical simulation demonstrated that CMCM method can detect the damage location and extent accurately, and has a good potential in structural health monitoring area.

For a structure, it is assumed that the mass and stiffness matrix (denoted as  $\mathbf{M}^*$  and  $\mathbf{K}^*$ , respectively) of the actual (experimental) model is a modification of the corresponding parameters (denoted as  $\mathbf{M}$  and  $\mathbf{K}$ , respectively) of the structural finite-element model (FEM), as shown that

$$\begin{cases} \mathbf{K}^* = \mathbf{K} + \sum_{n=1}^{N_e} \alpha_n \mathbf{K}_n^e \\ \mathbf{M}^* = \mathbf{M} + \sum_{n=1}^{N_e} \beta_n \mathbf{M}_n^e \end{cases} \quad (1)$$

where  $\mathbf{K}_n^e$ ,  $\mathbf{M}_n^e$  are the  $n$ th element stiffness and mass matrix, respectively;  $N_e$  is total number of elements;  $\alpha_n$ ,  $\beta_n$  are the  $n$ th element stiffness and mass correction coefficients to be determined, respectively. For CMCM model updating algorithm, the structural FEM parameters, including the mass matrix  $\mathbf{M}$  and stiffness matrix  $\mathbf{K}$ , can be updated or corrected using the modal measurements, including a few mode shapes and corresponding modal frequencies. Thus, the structural updating equation using the CMCM algorithm can be expressed as

$$\sum_{n=1}^{N_e} \alpha_n C_{n,ij} + \sum_{n=1}^{N_e} \beta_n E_{n,ij} = f_{ij} \quad (2)$$

in which

$$\begin{cases} C_{n,ij} = \boldsymbol{\varphi}_i^T \mathbf{K}_n \boldsymbol{\varphi}_j^* \\ E_{n,ij} = -\lambda_j^* \boldsymbol{\varphi}_i^T \mathbf{M}_n \boldsymbol{\varphi}_j^* \\ f_{ij} = \lambda_j^* \boldsymbol{\varphi}_i^T \mathbf{M} \boldsymbol{\varphi}_j^* - \boldsymbol{\varphi}_i^T \mathbf{K} \boldsymbol{\varphi}_j^* \end{cases} \quad (3)$$

where  $\boldsymbol{\varphi}_i$  denotes the  $i$ th eigenvector of the initial FEM model,  $\boldsymbol{\varphi}_j^*$  and  $\lambda_j^*$  mean the  $j$ th eigenvector and eigenvalue of the actual structure, respectively. When  $N_i$  modes, including their modal information, are available from the FEM model, and  $N_j$  modes are collected and computed by the measurement of actual structure, so totally  $N_m = N_i \times N_j$  CMCM equations can be available in Eq. (2). Using a new index  $m$  to replace  $ij$ , Eq. (2) can be re-written as

$$\sum_{n=1}^{N_e} \alpha_n C_{n,m} + \sum_{n=1}^{N_e} \beta_n E_{n,m} = f_m \quad (4)$$

written in a matrix form, one has

$$\mathbf{G}\boldsymbol{\gamma} = \mathbf{f} \quad (5)$$

where  $\mathbf{G} = [\mathbf{C} \ \mathbf{E}]$ ,  $\boldsymbol{\gamma} = [\boldsymbol{\alpha} \ \boldsymbol{\beta}]^T$ , in which,  $\mathbf{C}$  and  $\mathbf{E}$  are  $N_m \times N_e$  matrix,  $\boldsymbol{\alpha}$  and  $\boldsymbol{\beta}$  are column vector of size  $N_e$ , and  $\mathbf{f}$  is a column vector of size  $N_m$ . According to the CMCM algorithm, if  $N_m$  is greater than  $2N_e$ , more equations are available than unknowns, one would expect that a least-squares solution for  $\boldsymbol{\gamma}$  can be taken. According Hu and Li's study, to gain a unique solution for the correction factor, at least an additional constraint equation must be imposed. For instance, a particular mass or stiffness is predetermined, or the total mass of the system is known, etc.

## 2.2 Structural frequency-change-square-ratio based method

Frequency-change-square-ratio based method was first presented by Cawley and Adams (1979) in 1980s as a damage feature for structural health monitoring. Then, Hearn and Testa (1991) further demonstrated that the magnitude of change in natural frequencies is a function of the severity and of the location of deterioration in structures. Ratios of changes in natural frequencies are independent of severity for small deterioration and can serve to indicate the location of deterioration directly.

In the frequency-change-square-ratio based method, damage of the original structure is assumed to cause changes in the stiffness matrix by an amount  $\Delta\mathbf{K}$ . Distress in civil engineering structures may often have a significant effect on stiffness, but not on mass, so it is further assumed that the damage is not accompanied by a change in mass. The change in stiffness produces changes in eigenvalues  $\Delta\omega_i^2$  and eigenvectors  $\Delta\boldsymbol{\varphi}_i$ . The eigenvalue problem of the damage structure is given by

$$[(\mathbf{K} + \Delta\mathbf{K}) - (\omega^2 + \Delta\omega_i^2)\mathbf{M}](\boldsymbol{\varphi}_i + \Delta\boldsymbol{\varphi}_i) = 0 \quad (6)$$

Neglecting second-order terms, Eq. (6) leads to

$$\Delta\omega_i^2 = \frac{\boldsymbol{\varphi}_i^T \Delta\mathbf{K} \boldsymbol{\varphi}_i}{\boldsymbol{\varphi}_i^T \mathbf{M} \boldsymbol{\varphi}_i} \quad (7)$$

Assuming the structural stiffness changes  $\Delta\mathbf{K}$  was only induced by the change of the  $n$ th element stiffness  $\mathbf{K}_n$ , i.e.,  $\Delta\mathbf{K} = \Delta\mathbf{K}_n = \alpha_n \mathbf{K}_n$ , in which,  $\alpha_n$  means the proportional change in the stiffness of  $n$ th element. Then, Eq. (7) can be re-written as

$$\Delta\omega_i^2 = \frac{\alpha_n \boldsymbol{\varphi}_i^T \mathbf{K}_n \boldsymbol{\varphi}_i}{\boldsymbol{\varphi}_i^T \mathbf{M} \boldsymbol{\varphi}_i} \quad (8)$$

In Eq. (8), the change in natural frequencies still depends both on damage severity and on damage location. However, if Eq. (8) is written for two vibration modes  $i$  and  $j$ , and the ratio of frequency changes is formed, it is seen that this ratio is a function of damage location only, as shown as

$$\frac{\Delta\omega_i^2}{\Delta\omega_j^2} = \frac{\boldsymbol{\varphi}_i^T \mathbf{K}_n \boldsymbol{\varphi}_i}{\boldsymbol{\varphi}_j^T \mathbf{K}_n \boldsymbol{\varphi}_j} \quad (9)$$

To monitor the structural status, natural vibration frequencies are measured periodically. When changes in natural frequencies are observed, the set of ratios of changes is formed and is compared to the various member characteristic ratio ensembles obtained from Eq. (9). The location of damage is determined by selecting the member characteristic ensemble that most closely match the observed ratios of frequency changes of actual structure.

## 2.3 Evaluation criterion for the frequency change-square-ratio vectors

According to the description above, for frequency-change-square-ratio based method, one of the important procedure is to select the characteristic ensemble that most closely match between the measured and the characteristic frequency-change-ratios. So Modal Assurance Criterion (MAC) (Allemang 2003, Lieven and Ewins 1988, Ewins 2000) and Normalized Modal Difference (NMD) (Yang and Griffin 1997, Adewuyi and Wu 2015) methods were employed here to quantify and evaluate the similarity between the frequency-change-square-ratios.

Assuming the frequency-change-square-ratio (FCSR) vector  $\mathbf{F}$ , as a characteristic ensemble came from the structural FEM model, can be expressed as

$$\mathbf{F} = \left[ \frac{\Delta\omega_i^2}{\Delta\omega_k^2}, \frac{\Delta\omega_j^2}{\Delta\omega_k^2}, \dots, \frac{\Delta\omega_n^2}{\Delta\omega_k^2} \right]^T \quad (10)$$

where  $\Delta\omega_i^2$ ,  $\Delta\omega_j^2$ ,  $\Delta\omega_n^2$ ,  $\Delta\omega_k^2$  denote the  $i$ th,  $j$ th,  $n$ th,  $k$ th modal frequency-change-square, respectively. Similarly, the corresponding FCSR vector  $\tilde{\mathbf{F}}$  calculated from actual structural measurement can be written as

$$\tilde{\mathbf{F}} = \left[ \frac{\Delta\tilde{\omega}_i^2}{\Delta\tilde{\omega}_k^2}, \frac{\Delta\tilde{\omega}_j^2}{\Delta\tilde{\omega}_k^2}, \dots, \frac{\Delta\tilde{\omega}_n^2}{\Delta\tilde{\omega}_k^2} \right]^T \quad (11)$$

Ewins (1988, 2000) proposed the Modal Assurance Criterion (MAC) method to quantify the similarity between two independent mode shapes. In this study, the MAC method was also employed to evaluate the similarity between the measured and the characteristic FCSR vectors, so the corresponding equation can be expressed as

$$\text{MAC}(\mathbf{F}, \tilde{\mathbf{F}}) = \frac{\mathbf{F}^T \tilde{\mathbf{F}}}{\sqrt{(\mathbf{F}^T \mathbf{F})(\tilde{\mathbf{F}}^T \tilde{\mathbf{F}})}} \quad (12)$$

where  $\mathbf{F}$  and  $\tilde{\mathbf{F}}$  represent the frequency-change-square-ratio (FCSR) vectors of the characteristic and the measured model, respectively. Ewins (2000) demonstrated that when  $\text{MAC} > 0.9$ , these two mode shapes can be regarded as have a good correlation. When  $\text{MAC} < 0.05$ , these two mode shapes is irrelevant.

Normalized Modal Difference (NMD) is another evaluation method, which can be expressed as

$$\text{NMD}(\mathbf{F}, \tilde{\mathbf{F}}) = \sqrt{\frac{1 - \text{MAC}(\mathbf{F}, \tilde{\mathbf{F}})}{\text{MAC}(\mathbf{F}, \tilde{\mathbf{F}})}} \quad (13)$$

Compared to MAC, the NMD is more sensitive to the similarity. The closer to 1 for MAC, or the closer to 0 for NMD, the more similar for these two FCSRs.

### 3. FCSR-based damage detection for shear buildings

After the related theoretical foundations were briefly described, this section focused on the theoretical derivation and detail procedure description of the developed method. At first, the typical physical parameters distribution characteristic of shear buildings was introduced. Then, based on this typical element stiffness and mass distribution, the FCSR baseline dataset was constructed combining with the CMCM algorithm. At last, the detail procedure of this damage detection method was summarily presented in the section.

#### 3.1 Typical parameters distribution characteristic of shear buildings

For shear structures as shown in Fig. 1, the mass of the  $i$ th floor can be denoted as  $m_i$ , then the corresponding system mass matrix  $\mathbf{M}$  is written as  $\mathbf{M} = \sum_{i=1}^n \mathbf{M}_i^e = \text{diag}(m_1, m_2, \dots, m_{n-1}, m_n)$ , in which,  $\mathbf{M}_i^e$  denotes the corresponding  $m_i$  represented in the global coordinates.

Similarly, the lateral stiffness of the  $i$ th story can be denoted as  $k_i$ , and the corresponding element stiffness matrix  $\mathbf{k}_i^e$  in the global coordinates can be written as  $\mathbf{K}_i^e$ , then, the system stiffness matrix  $\mathbf{K}$  for the  $n$ -story shear building can be assembled as

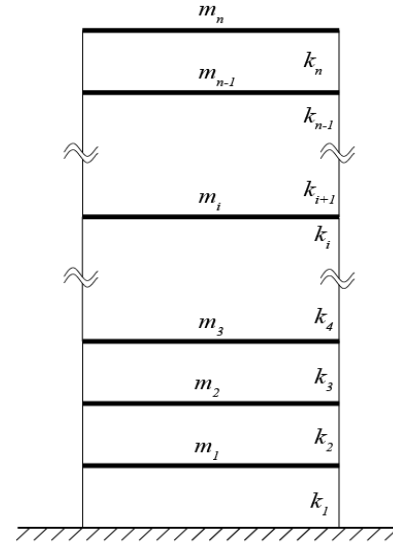


Fig. 1 Diagram of an  $n$ -story shear building

$$\mathbf{K} = \sum_{i=1}^n \mathbf{K}_i^e \begin{bmatrix} k_1 + k_2 & -k_2 & 0 & \cdots & 0 \\ -k_2 & k_2 + k_3 & -k_3 & 0 & \vdots \\ 0 & -k_3 & \ddots & \ddots & 0 \\ \vdots & 0 & \ddots & k_{n-1} + k_n & -k_n \\ 0 & \cdots & 0 & -k_n & k_n \end{bmatrix} \quad (14)$$

Based on above analysis, the corresponding eigenvalue  $\lambda$  and eigenvector  $\boldsymbol{\varphi}$  of the shear structure could be calculated by eigenvalue decomposition of structure mass matrix  $\mathbf{M}$  and stiffness matrix  $\mathbf{K}$ , which are established by the mass vector  $\mathbf{m} = [m_1, m_2, \dots, m_n]$  and stiffness vector  $\mathbf{k} = [k_1, k_2, \dots, k_n]$  in the way mentioned above.

#### 3.2 Construction of the FCSR baseline dataset of shear buildings

For structural damage detection of shear buildings, Liang *et al.* (2017) proposed a new concept using structural element mass-stiffness vector (SEMV) based on the typical mass and stiffness distribution characteristics of shear buildings. In Liang's study, a corresponding damage identification method was developed by combining SEMV with the cross-model cross-mode (CMCM) model updating algorithm. As a result, the structural damage location and severity can be identified accurately, even only the structural acceleration measurements are provided. Based on this distinguish feature, concept of the SEMV-based approach will be employed to help to form the developed method of this paper, so a brief description of this method is introduced in the following.

At first, according to the CMCM algorithm described in section 2.1, the complete model updating for all mass and stiffness parameters can be realized when only one constraint is available. So, it is first assumed that  $m_1$  is known as the necessary constraint, then the mass and stiffness vectors of shear structures can be re-written as

$$\begin{cases} \tilde{\mathbf{m}} = [m_1, \hat{m}_2, \hat{m}_3, \dots, \hat{m}_n] \\ \tilde{\mathbf{k}} = [\hat{k}_1, \hat{k}_2, \hat{k}_3, \dots, \hat{k}_n] \end{cases} \quad (15)$$

where  $\hat{m}_i, \hat{k}_i$  ( $i=1,2,\dots,n$ ) mean the mass and stiffness values of the initial to-be-updated model, respectively. According to the typical characteristics of shear buildings described in last section, if this to-be-updated model exists, all the structural parameters, including the corresponding mass matrix  $\tilde{\mathbf{M}}$ , stiffness matrix  $\tilde{\mathbf{K}}$ , element mass and stiffness matrix  $\tilde{\mathbf{M}}_i^e, \tilde{\mathbf{K}}_i^e$  ( $i = 1,2,\dots,n$ ) expressed in the global coordinates, eigenvalue  $\hat{\lambda}$  and eigenvector  $\hat{\boldsymbol{\varphi}}$  of the given to-be-updated model, could be obtained by assembling or calculating. Consequently, all the element stiffness and mass correction coefficients  $\hat{\boldsymbol{\alpha}}, \hat{\boldsymbol{\beta}}$  of the to-be-updated model could also be calculated following the CMCM algorithm by combining with the actual measured modal information of the structure.

Therefore, the updated mass and stiffness of the model can be expressed as

$$\begin{cases} m_i = m_1 \\ m_i = \hat{m}_i(1 + \hat{\beta}_i), (i = 2,3,\dots,n) \\ k_i = \hat{k}_i(1 + \hat{\alpha}_i), (i = 1,2,3,\dots,n) \end{cases} \quad (16)$$

where  $m_i$  and  $k_i$  denote the updated element mass and stiffness, respectively, which equal to actual structural physical parameters. Thus, based on above theoretical analysis, a conclusion could be summarized, although the given initial models may differ in their spatial and modal properties ( $\tilde{\mathbf{K}}, \tilde{\mathbf{M}}, \tilde{\mathbf{K}}_i^e, \tilde{\mathbf{M}}_i^e, \hat{\boldsymbol{\varphi}}, \hat{\lambda}$ ), with the help of CMCM method by combining with the corresponding stiffness and mass correction factors  $\hat{\boldsymbol{\alpha}}, \hat{\boldsymbol{\beta}}$ , the final updated model is the same ( $\mathbf{K}, \mathbf{M}, \mathbf{K}_i^e, \mathbf{M}_i^e, \boldsymbol{\varphi}, \lambda$ ) with actual modal measurement, i.e., no matter what the initial given model is, the physical parameters of an actual structure could be obtained after model updating according to Eq. (16). In other words, the final updated model is less susceptible to the assumed values of initial  $\hat{m}_i, \hat{k}_i$ , and the given model could finally be corrected or updated to true structural element mass and stiffness using the CMCM algorithm.

Based on above analysis, assuming all the element mass and stiffness of a given to-be-updated model equal to  $m_1$ , i.e.,  $\hat{m}_i = m_1, \hat{k}_i = m_1$ , then the updated mass and stiffness, denoted as the vector form  $\mathbf{Z}=[m_1, m_2, \dots, m_n, k_1, k_2, \dots, k_n]$ , can be expressed as

$$\mathbf{Z} = m_1 \mathbf{U}_{m_1} \quad (17)$$

where

$$\mathbf{U}_{m_1} = [1, (1 + \tilde{\beta}_2), (1 + \tilde{\beta}_3), \dots, (1 + \tilde{\beta}_n), (1 + \tilde{\alpha}_1), (1 + \tilde{\alpha}_2), \dots, (1 + \tilde{\alpha}_n)] \quad (18)$$

in which, vector  $\mathbf{U}_{m_1}$  can be regarded as the normalization of vector  $\mathbf{Z}$  at the location of  $m_1$ , i.e.,  $1 + \tilde{\beta}_i = m_i/m_1, 1 + \tilde{\alpha}_j = k_j/m_1$  ( $i=2,3,\dots,n, j = 1,2,\dots,n$ ). In addition, it should be noted that the  $\mathbf{U}_{m_1}$  calculation is based on the assumption that  $m_1$  has been pre-determined, however, the final value of  $\mathbf{U}_{m_1}$  has nothing to do with  $m_1$  because  $\mathbf{U}_{m_1}$  is just

normalized at  $m_1$  location. Thus, the vector  $\mathbf{U}_{m_1}$  in Eq. (18) can be explained as  $m_1$ -normalized structural element mass-stiffness vector (SEMV). Finally, a conclusion can be drawn that the SEMV vector of a structure represents the structural particular mass and stiffness distribution in certain sequence, therefore, as the inherent property of an actual structure, it can be used for damage detection.

On the other hand, according to the procedures mentioned above,  $m_1$  in SEMV  $\mathbf{U}_{m_1}$  can be any positive constant for a given to-be-updated model, in which  $\hat{m}_i = m_1, \hat{k}_i = m_1$  ( $i=1,2, \dots, n$ ). Then, the corresponding SEMV can be obtained by substituting the correction coefficients  $\tilde{\boldsymbol{\alpha}}, \tilde{\boldsymbol{\beta}}$  of the to-be-updated model into Eq. (18) after the CMCM model updating calculation. Likewise, if assuming another parameter of the structure has been pre-determined (such as  $k_1$ ), all the previous theoretical analysis and conclusion can still work, and the only difference is that the element value corresponding to  $k_1$  has changed to 1 in the  $k_1$ -normalized SEMV.

### 3.3 The detail procedure of the developed damage detection method

For the developed damage detection method, which combined the cross-model cross-mode (CMCM) model updating algorithm with the structural frequency-change-square-ratio based method, as shown in Fig. 2, the detail procedure can be summarized as following:

(1) Assuming the initial to-be-updated model. Following the description in section 3.2, an initial to-be-updated model corresponding to the actual shear structure is established, in which,  $m_1$  is chosen randomly (here 1 is chosen only for the convenient of demonstration purpose) and other parameters equal to  $m_1$  consistently ( $\hat{m}_i = m_1, \hat{k}_i = m_1$ ). The corresponding parameters of this model, including  $\tilde{\mathbf{K}}, \tilde{\mathbf{M}}, \tilde{\mathbf{K}}_i^e, \tilde{\mathbf{M}}_i^e, \hat{\boldsymbol{\varphi}}, \hat{\lambda}$ , are subsequently constructed and calculated.

(2) Updating the initial model. By analyzing the measured acceleration of actual structure under the health condition, the first several modal information, including the modal frequencies and mode shapes, can be obtained. Then, the assumed initial to-be-updated model can be updated using the CMCM algorithm combining with the obtained modal information of actual structure.

(3) Building the actual FCSR vector. The first several modal frequencies of actual structure under the test condition can be obtained by analyzing the acceleration measurement, then the corresponding structural frequency-change-square-ratio (FCSR) vector can be formed by combining the structural frequencies obtained at the health condition with the one obtained at the test condition.

(4) Building the FCSR baseline datasets of damage location. As described in section 3.2, the updated model in step (2) has the same modal information (modal frequency and mode shape) with the actual structure at health condition. Therefore, a FCSR baseline datasets of damage location can be constructed by artificially reducing the element stiffness of the updated model with a certain value one by one.

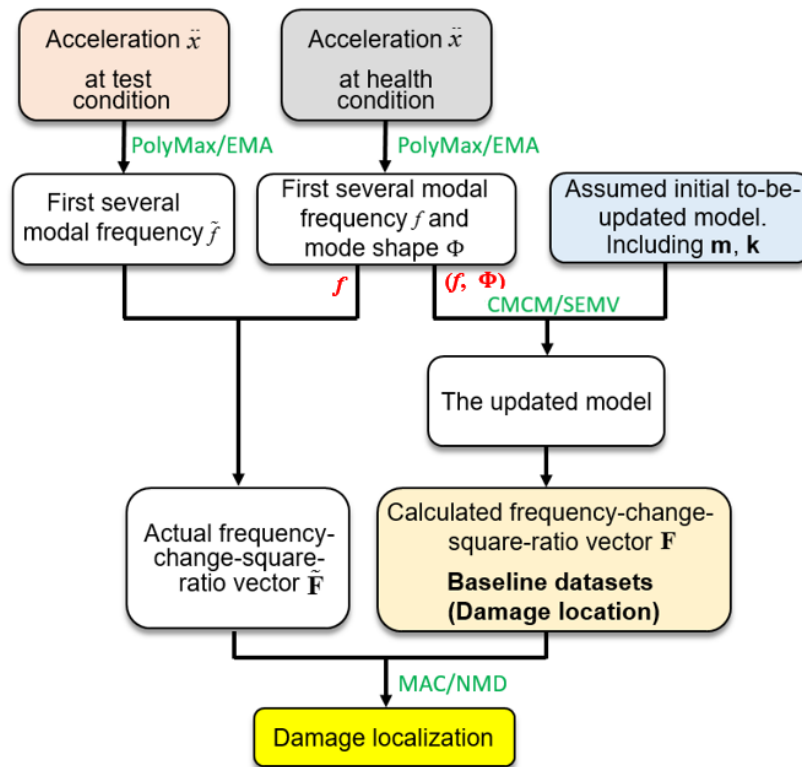


Fig. 2 Procedure of the developed damage detection method

(5) Damage localization. By calculating and comparing the the MAC and NMD values for the structural FCSRs, which came from the test condition in step (3) and the baseline datasets constructed in step (4), respectively, the damage location of the actual structure can be identified by selecting the most matched FCSR sample in the baseline. The corresponding preset damage location of this selected FCSR can be regarded as the actual structural damage location. The closer to 1 for MAC and to 0 for NMD, the more possibility for the actual damage locates in the pre-set location of the selected FCSR sample.

#### 4. Numerical simulation

In this section, a four-story shear building is studies as a numerical example to demonstrate the detailed procedure and to verify the effectiveness of the developed method.

##### 4.1 Model introduction

Assuming a four-story shear building, as shown in Fig. 1 and considered  $n = 4$ , its uniform mass and inter-story stiffness distribution along the height of the structure is known, *i.e.*,  $m_1 = m_2 = m_3 = m_4 = 1.0 \times 10^5$  kg and  $k_1 = k_2 = k_3 = k_4 = 2.04 \times 10^8$  N/m, and each floor slab can only move horizontally. In order to obtain the acceleration measurement of the building under ambient excitation, four accelerometers were attached to each floor slab with a sampling frequency of 320 Hz. At the same time, four

uncorrelated band-limited white noise with a bandwidth of 0 Hz to 50 Hz, were applied to each floor slab to simulate ambient excitations. In this study, the corresponding structural dynamic responses including accelerations, velocities and displacement, which can be regarded as the exact response under ambient excitation, were simulated by using the discrete-time state space model (Juang 1994) technique.

In order to verify the effectiveness of the developed damage detection method, nine different scenarios were introduced for this numerical model, as shown in Table 1, in which, the stiffness of each floor was reduced 15% and 30%, respectively. For each scenario, the test lasted 25.6s, *i.e.*, 8192 samples were recorded. In addition, white noise with 5 percent Signal-to-Noise Ratio (SNRs), *i.e.*,  $SNR = 5\%$ , is mixed into the "measured" (simulated) acceleration signals to test the robustness ability of the proposed approach. Fig. 3 presents the collected "measured" acceleration signal in time domain and its power spectrum density in frequency domain. Because of the space limitation, only channel 2 was presented in the figure.

After the acceleration signals of each floor were measured, the corresponding structural modal parameters, including modal frequencies and mode shapes, for different test conditions can be obtained by using various existing modal parameter identification algorithm. In the study, a commercial modal analysis and calculating software, LMS test lab (Zhang *et al.* 2008), was employed here to help to identify and extract the structural modal information from the measured acceleration. For this software, the core

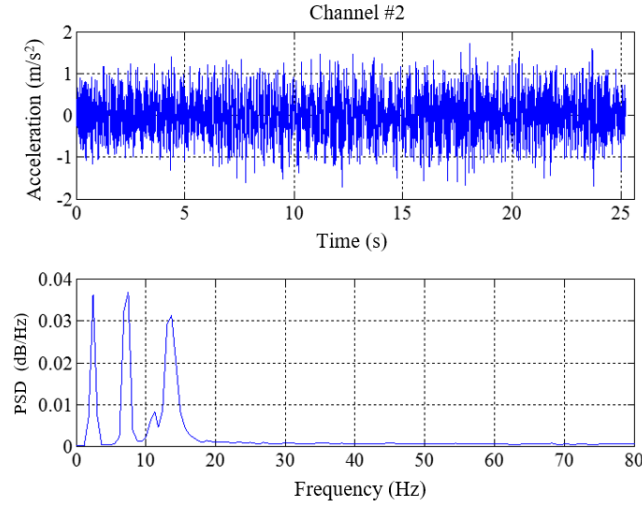


Fig. 3 The acceleration time-history and its power spectrum density

Table 1 Summary of structure state conditions.

Scenarios	K1	K2	K3	K4
State#1	--	--	--	--
State#2	-15%	--	--	--
State#3	-30%	--	--	--
State#4	--	-15%	--	--
State#5	--	-30%	--	--
State#6	--	--	-15%	--
State#7	--	--	-30%	--
State#8	--	--	--	-15%
State#9	--	--	--	-30%

Table 2 The first four frequencies of the structure under nine different conditions. (Unit: Hz)

Order	State#1	State#2	State#3	State#4	State#5	State#6	State#7	State#8	State#9
1	2.48	2.41	2.29	2.43	2.33	2.46	2.40	2.49	2.47
2	7.21	7.00	6.78	7.19	7.19	6.99	6.73	6.98	6.67
3	11.05	10.86	10.72	10.69	10.27	10.96	10.89	10.64	10.25
4	13.51	13.46	13.42	13.20	12.96	13.08	12.69	13.35	13.23

Table 3 The updated physical parameters for the initial assumed to-be-updated model.

	Actual physical parameters	Assumed initial parameters	No noise		SNR = 5%	
			Correction coefficients	Updated parameters	Correction coefficients	Updated parameters
$m_1$	$1.0 \times 10^5$	1	--	1	--	1
$m_2$	$1.0 \times 10^5$	1	0.0679	1.0679	-0.0672	0.9328
$m_3$	$1.0 \times 10^5$	1	0.0860	1.0860	-0.0946	0.9054
$m_4$	$1.0 \times 10^5$	1	0.0891	1.0891	-0.0563	0.9437
$k_1$	$2.04 \times 10^8$	1	$2.0681 \times 10^3$	$2.0691 \times 10^3$	$2.0392 \times 10^3$	$2.0402 \times 10^3$
$k_2$	$2.04 \times 10^8$	1	$2.0739 \times 10^3$	$2.0749 \times 10^3$	$1.9670 \times 10^3$	$1.9680 \times 10^3$
$k_3$	$2.04 \times 10^8$	1	$2.1652 \times 10^3$	$2.1662 \times 10^3$	$1.9080 \times 10^3$	$1.9090 \times 10^3$
$k_4$	$2.04 \times 10^8$	1	$2.1998 \times 10^3$	$2.2008 \times 10^3$	$1.9255 \times 10^3$	$1.9265 \times 10^3$

\* all the unit of the element mass is kg, and the unit of the element stiffness is N/m

Table 4 The frequency-change-square-ratio for each reduction conditions of the structure

	$k_1$ (-20%)		$k_2$ (-20%)		$k_3$ (-20%)		$k_4$ (-20%)	
	$F^*$	F	$F^*$	F	$F^*$	F	$F^*$	F
$\Delta\lambda_2/\Delta\lambda_1$	5.99	6.14	0	0	14.24	12.90	52.18	45.37
$\Delta\lambda_3/\Delta\lambda_1$	7.06	6.94	20.13	20.35	5.66	4.10	132.85	117.77
$\Delta\lambda_4/\Delta\lambda_1$	2.80	2.40	21.71	19.64	53.56	52.23	67.69	67.62

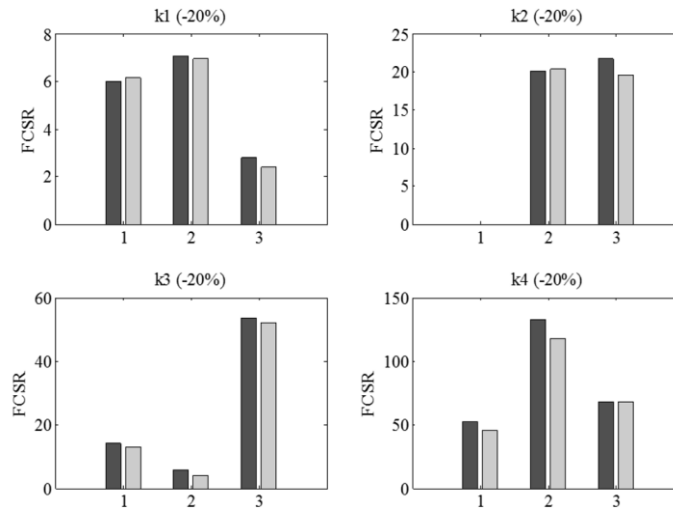


Fig. 4 The FCSRs calculated from the updated model and actual structures, in which, the bar with dark color denotes the FCSR calculated by the actual structural physical parameters, and the bar with light color denotes the FCSR calculated based on the updated model

identification algorithm is called PolyMax (Peeters *et al.* 2004 a, b), which is a non-iterative frequency-domain parameters estimation method and presents very good stability, accuracy of the estimated modal parameters and quality of the frequency response function synthesis when compared with classical Experimental Modal Analysis (EMA) method (Cuuha and Caetano 2006, Maia and E Silva 1997). Therefore, the modal frequency identification results for these nine test scenarios in this section can be achieved, as shown in Table 2.

#### 4.2 Construction of the FCSR baseline dataset

For this numerical model under health condition, its modal parameters, including the modal frequencies and mode shapes, were obtained by using the modal parameters identification algorithm, for example, by employing the LMS test lab software. Then, assuming a to-be-updated model for this numerical structure existed, and its element mass  $m_1$  had been known (here 1 is chosen only for the convenient of calculation) and other parameters were all equal to  $m_1$  consistently, *i.e.*,  $\hat{m}_i = 1$ ,  $\hat{k}_i = 1$  ( $i=1,2,\dots,n$ ). Following the description in section 3.2, this to-be-updated model with the initial physical parameters can be updated using the CMCM algorithm by combining with the identified frequencies of the actual structure under health condition. Table 3 presents the correction coefficients and the updated physical parameters.

After the updated physical parameters of the assumed initial model were obtained, the corresponding updated model can be re-constructed based on the typical element mass and stiffness distribution characteristic of shear buildings, as described in section 3.1 and 3.2. Then, in order to build the FCSR baseline datasets of damage location for this numerical model, the element stiffness of this updated model was artificially reduced at 20% one by one, and then for each stiffness reduction scenario, its corresponding modal frequencies can be calculated by modal analysis process. Finally, the frequency-change-square-ratio  $F$ , *i.e.*,  $\Delta\lambda_i/\Delta\lambda_1$  ( $i=2,3,4$ ) as shown in Table 4, for each reduction scenario can be obtained by combining with the structural frequencies under the health condition. At the same time, the actual structural FCSRs denoted as  $F^*$  in Table 4, were also calculated from the actual structural physical parameters. In order to further analyze the difference between  $F$  and  $F^*$ , a bar figure was presented in Fig. 4.

From Table 4 and Fig. 4, it is clear that the FCSRs calculated from the updated model, have a good consistency with the one calculated based on the actual structure. This result demonstrates that the model, which was updated from the assumed initial structural physical parameters by combining with the actual structural frequencies, can be employed as a representation of the FEM model of the actual shear structure in some degree, because they share a very similar modal parameters, including modal frequencies

Table 5 The FCSRs calculated by the measured frequencies of actual structure

	State#2	State#3	State#4	State#5	State#6	State#7	State#8	State#9
$\Delta\lambda_2/\Delta\lambda_1$	6.10	5.74	0	0	14.48	13.67	52.59	50.83
$\Delta\lambda_3/\Delta\lambda_1$	7.37	6.45	20.06	20.04	5.63	5.72	140.83	115.61
$\Delta\lambda_4/\Delta\lambda_1$	2.97	2.48	23.50	18.37	57.30	46.21	75.58	53.75

Table 6 The damage location identification results based on the FCSRs based method

	ID	State#2	State#3	State#4	State#5	State#6	State#7	State#8	State#9
MAC	1	1.00	1.00	0.66	0.70	0.47	0.50	0.92	0.95
	2	0.74	0.71	1.00	1.00	0.74	0.75	0.91	0.88
	3	0.49	0.47	0.79	0.71	1.00	1.00	0.57	0.53
	4	0.94	0.92	0.89	0.93	0.61	0.64	1.00	1.00
NMD	1	0.04	0.02	0.72	0.65	1.07	0.99	0.30	0.24
	2	0.60	0.64	0.07	0.02	0.60	0.58	0.31	0.37
	3	1.02	1.05	0.52	0.64	0.01	0.04	0.86	0.94
	4	0.26	0.29	0.35	0.28	0.80	0.76	0.02	0.07

and mode shapes. On the other hand, the permutation and combination of the FCSRs in Fig. 4 are very different with each other for these four stiffness reduction scenarios, and this phenomenon can be attributed to the difference of the damage location. All the results predicted that the structural FCSRs have a good potential ability to identify the damage location.

#### 4.3 Damage localization

After the FCSRs of the updated model with different damage location were calculated and analyzed, then the FCSR baseline datasets of the damage location can be constructed for this actual structure, as shown in Table 4. At the same time, the actual FCSRs, which were calculated by the measured frequencies of actual structure, can also be obtained for these eight test conditions, as shown in Table 5. Then, by calculating the MAC and NMD value to compare the similarity of the actual structural FCSRs with the one came from the baseline datasets, a special FCSR sample, which has the maximum MAC value and minimum NMD value, can be selected from the baseline datasets. At last, the preset element damage location corresponding to this selected FCSR sample, can be regarded as the actual damage location of the test structure, and all the identification results were shown in Table 6.

From Table 6, it is clear that the damage location of these eight test conditions can be identified accurately, because the selected FCSRs sample has the maximum MAC value, i.e.,  $MAC = 1$ , and the minimum NMD value, i.e.,  $NMD \approx 0$ . All the simulation results demonstrate that the developed method of this paper has a good ability to realize the damage localization, even only the first several frequencies were provided.

## 5. LANL test-bed structure

In this section, experimental tests at Los Alamos National Laboratory (LANL) are employed to validate the damage detection and localization ability and to illustrate the application of the developed method.

### 5.1 Model description

As shown in Fig. 5, the LANL three-story shear-building consists of four aluminum plate ( $30.5 \text{ cm} \times 30.5 \text{ cm} \times 2.5 \text{ cm}$ ), which were connected by bolted joints to four aluminum columns ( $17.7 \text{ cm} \times 2.5 \text{ cm} \times 2.5 \text{ cm}$ ) at each floor. It should be noted that an additional element ( $15 \text{ cm} \times 2.5 \text{ cm} \times 2.5 \text{ cm}$ ) attached to the top floor and an adjustable bumper mounted on the second floor, were used to introduce a gap nonlinearity in the system, and the gap distance can be modified by adjusting the position of the bumper to vary the level of the nonlinearity. At the beginning, the gap distance was adjusted large enough to guarantee the system within the linear range during the dynamic tests conducted in this study. The whole structure was mounted on two rails to allow the system to slide only in one direction, and an electro-dynamic shaker was used to provide a band-limited random base excitation (20-150Hz) to the test structure (Figueiredo *et al.* 2009).

For the structure, four accelerometers with nominal sensitivities of 100 mv/g, were attached to each aluminum plate along a vertical center line to measure the dynamic response of the 4DOF lab structure. In addition, a force transducer with nominal sensitivities of 2.2 mV/N, was connected to the tip of the stinger to gauge the input force generated by the shaker. All the sensor's measurement were recorded at a sampling frequency of 322.58Hz by a data acquisition system. Full details concerning the LANL test setup are documented in Figueiredo's research (Figueiredo *et al.* 2009).

Table 7 Summary of the structural state conditions

Label	Condition	Description
State#1	Reference condition	Health
State#2	21.5% 1 <sup>st</sup> -story stiffness reduction	Exchange one column on the 1 <sup>st</sup> -story
State#3	21.5% 2 <sup>nd</sup> -story stiffness reduction	Exchange one column on the 2 <sup>nd</sup> -story
State#4	21.5% 3 <sup>rd</sup> -story stiffness reduction	Exchange one column on the 3 <sup>rd</sup> -story

Table 8 Identified modal frequencies and damping ratio of four states

Conditions	Frequency /(Hz)			Damping (%)		
	2nd	3rd	4th	2nd	3rd	4th
State#1	30.7	54.2	70.7	6.3	2.0	0.97
State#2	30.9	51.2	69.2	7.1	2.2	0.55
State#3	29.7	53.9	65.8	5.3	1.7	1.2
State#4	30.2	51.1	69.3	5.6	2.2	0.80

Table 9 The updated model using the CMCM algorithm

Actual physical parameters			$m_1$ -normalized	The updated result		
				Initial assumption	Correction coefficients	Updated parameters
$m_1$	6.54	1	1	1	--	1
$m_2$	6.66	1.0183	1	1	-0.0147	0.9853
$m_3$	6.86	1.0489	1	1	-0.0034	0.9966
$m_4$	6.80	1.0398	1	1	0.0758	1.0758
$k_1$	$4.0 \times 10^5$	$6.1131 \times 10^4$	1	1	$6.0455 \times 10^4$	$6.0456 \times 10^4$
$k_2$	$4.0 \times 10^5$	$6.1131 \times 10^4$	1	1	$5.8721 \times 10^4$	$5.8722 \times 10^4$
$k_3$	$4.0 \times 10^5$	$6.1131 \times 10^4$	1	1	$5.9494 \times 10^4$	$5.9495 \times 10^4$

\* all the unit of the element mass is kg, and the unit of the element stiffness is N/m



Fig. 5 LANL-4DOF test-bed structure experiment

In the study, three damage conditions were introduced by reducing the story's stiffness by 21.5%, which was realized by replacing the corresponding column with another one with half the cross-section thickness in the direction of shaking. The four structural state configurations considered in the study are summarized in Table 7.

For these four structural states in this study, the corresponding modal frequencies and damping ratio can be identified using ERA algorithm (Juang 1994), as summarized in Table 8. It should be noted that only the lower three modal frequencies from the experimental measurement are used in the following study.

## 5.2 Construction of the FCSR baseline dataset

As described in last section, the modal parameters (modal frequencies and mode shapes) of the structure under health condition can be obtained by analyzing the measured acceleration, as shown in Table 8. At the same time, following the detail procedure of the FCSR baseline construction described in section 3.3, assuming a to-be-updated model of this actual structure under health condition existed, and its physical parameters were all equal to one, i.e.,  $m_i = 1$ ,  $k_i = 1$  ( $i=1,2,\dots,4$ ) and  $m_1$  had been known. Thus, the other physical parameters, including the mass and stiffness matrix, of this to-be-updated model can be obtained according to the typical characteristic of the element mass-stiffness distribution of shear building. Then, by combining with the actual structural frequencies obtained under the health condition, this assumed initial to-be-updated model can be updated using the CMCM model

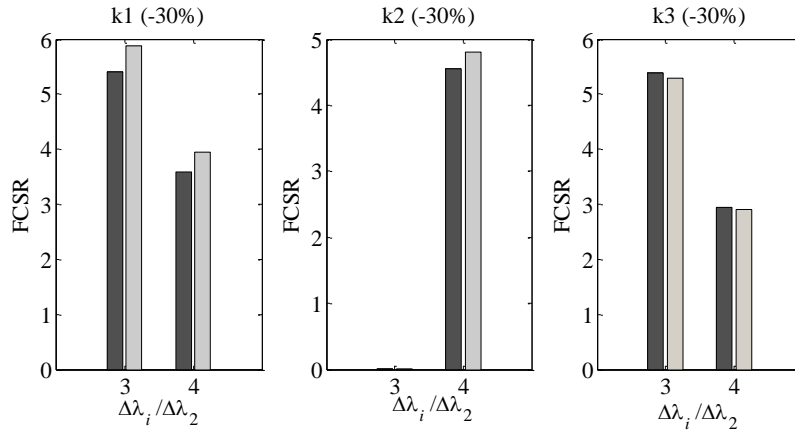


Fig. 6 Frequency-change-square-ratio (FCSR) of the baseline datasets, in which, the bar with dark color denotes the FCSR calculated by the actual structural physical parameters, and the bar with light color denotes the FCSR calculated based on the updated model

Table 10 The FCSR baseline dataset of damage location

	k <sub>1</sub> (-30%)		k <sub>2</sub> (-30%)		k <sub>3</sub> (-30%)	
	F*	F	F*	F	F*	F
$\Delta\lambda_3/\Delta\lambda_2$	5.4115	5.8781	0.0047	0.0134	5.3892	5.2858
$\Delta\lambda_4/\Delta\lambda_2$	3.5879	3.9544	4.5461	4.8031	2.9403	2.9041

Table 11 The actual FCSR under three different damage conditions

FCSR	State#2	State#3	State#4
$\Delta\lambda_3/\Delta\lambda_2$	-25.67	0.54	10.72
$\Delta\lambda_4/\Delta\lambda_2$	-17.03	11.07	6.44

updating algorithm, and the updated results were presented in Table 9. From the Table, it is clear that the physical parameters of the updated model have a good consistency with the actual structural parameters after having been normalized on  $m_1$ .

This updated model can be regarded as the representation of the FEM model for actual structure in some degree, because their modal parameters, including the modal frequencies and mode shapes, are almost the same. Therefore, based on this updated model, the FCSR baseline dataset of the damage location of actual structural can be constructed by artificially reducing the element stiffness at 30% one by one for the updated model, and then the corresponding modal frequencies for each stiffness reduction conditions can be calculated. Finally, the FCSR for each reduction scenario can be obtained by combining with the structural frequencies on health condition, as shown in Table 10, in which, F denotes the FCSR of the baseline dataset calculated based on the updated model, and F\* denotes the FCSR calculated based on actual structural physical parameters. From Table 10 and Fig. 6, a good consistency can be observed for FCSRs, which were calculated based on the updated model and the actual structural parameters, respectively. This results demonstrate that the updated model using the developed method can be

effectively employed to represent the FEM of actual structure to attend the FCSR-based damage detection procedure. On the other hand, it should be noted that the FCSRs in the location of  $k_1$  and  $k_3$  in Table 10 are almost the same, this phenomenon may be caused by the symmetry characteristic of the test structure along the vertical direction. When the symmetry exists for the test structure, the frequency-based damage detection technique may lost its effectiveness, because it cannot have the ability to distinguish which side the damage locates. Lots of research and the following identification results also validate this conclusion.

### 5.3 Damage localization

The FCSRs of the actual structure under three different damage conditions can be calculated by combining the frequencies obtained from the corresponding damage condition with the one obtained from the health condition, and the result was presented in Table 11. Then, for each damage condition, its actual FCSR will be compared with the one selected from the constructed baseline dataset for their similarity using the MAC and NMD method.

Table 12 The damage location identification results using the developed method.

	Floor	State#2	State#3	State#4
MAC	1	1.00	0.60	1.00
	2	0.56	1.00	0.52
	3	1.00	0.52	1.00
NMD	1	0.00	0.82	0.04
	2	0.90	0.03	0.97
	3	0.06	0.95	0.03

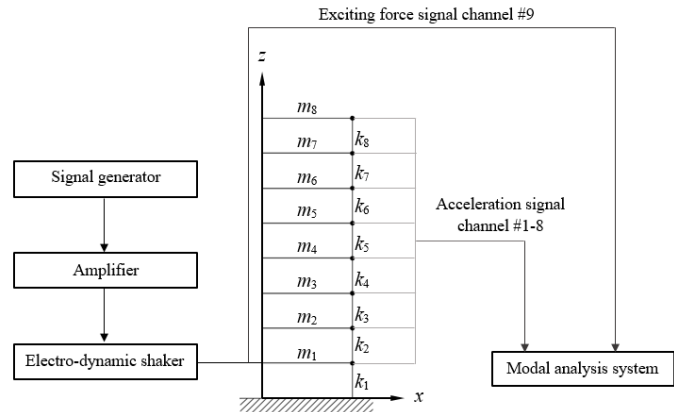
result.

Table 13 Summary of structure state conditions

Scenarios	State Condition	Description
State#1	Undamaged	Baseline condition
State#2	Damaged	8.3% stiffness reduction on the 1 <sup>st</sup> -story
State#3	Damaged	8.3% stiffness reduction on the 2 <sup>nd</sup> -story
State#4	Damaged	8.3% stiffness reduction on the 3 <sup>rd</sup> -story
State#5	Damaged	8.3% stiffness reduction on the 4 <sup>th</sup> -story
State#6	Damaged	8.3% stiffness reduction on the 5 <sup>th</sup> -story
State#7	Damaged	8.3% stiffness reduction on the 6 <sup>th</sup> -story
State#8	Damaged	8.3% stiffness reduction on the 7 <sup>th</sup> -story
State#9	Damaged	8.3% stiffness reduction on the 8 <sup>th</sup> -story



(a) The test model



(b) The sketch of the test

Fig. 7 The eight-story frame model

Finally, the most similar FCSR sample, which has the maximum MAC value and minimum NMD value, will be selected from the datasets, and its preset damage element location of the selected FCSR sample will be regarded as the actual damage location of the structure. The final identification result can be found in Table 12.

From Table 12, it is clear that with the maximum MAC = 1 and minimum NMD = 0.03, the damage location of the structure under State#3 can be identified accurately. However, for State#2 and State#4, they share a very similar detection result, the MAC value on 1<sup>st</sup> and 3<sup>rd</sup> floor all have the maximum value, i.e., MAC = 1, and all its corresponding NMD values are almost minimum. This result further validates the conclusion that the structural symmetry will affect the frequency-based identification

## 6. An eight-story frame-based test structure

In order to further validate the feasibility of the proposed FCSR-based damage detection method, another eight-story frame structure was experimentally tested and investigated in the laboratory. All the experimental data came from the school of aeronautics at Northwestern Polytechnical University, China, and it is greatly appreciated for their assistance and contribution.

### 6.1 Model description

An eight-story frame structure was designed and assembled in the laboratory, as shown in Fig. 7(a), and the neighboring layers of the structure were connected by

Table 14 Identified structural modal frequencies under the nine test conditions

Scenarios	1st	2nd	3rd	4th	5th	6th	7th	8th
State#1	2.36	7.46	11.95	16.20	20.08	23.12	25.37	26.87
State#2	2.35	7.39	11.88	16.15	20.02	23.10	25.36	26.86
State#3	2.36	7.47	11.99	16.22	19.93	22.86	25.22	26.88
State#4	2.35	7.48	11.88	15.99	20.00	22.93	25.00	26.86
State#5	2.36	7.49	11.90	16.27	19.90	23.09	25.31	26.96
State#6	2.36	7.44	11.99	16.00	20.08	22.79	25.35	26.74
State#7	2.36	7.42	11.97	16.15	19.86	22.97	25.39	26.57
State#8	2.36	7.43	11.85	16.08	20.04	22.93	25.18	26.51
State#9	2.34	7.40	11.86	15.95	19.74	22.72	25.11	26.55

four steel columns. Each column was assembled by stacking three steel sheets (139 mm × 27 mm × 1 mm) together, thus the bending stiffness of steel column is much larger in the y-direction (i.e., the width direction) than that in the x-direction (i.e., the thickness direction). Therefore, only the vibration in the x-direction was studied during the test. The frame structure was assumed to have a lumped mass on each layer and the inter-story stiffness distribution along the height of the columns.

As shown in Fig. 7(b), an electro-dynamic shaker provided a lateral band-limited sine sweeping excitation (0~50 Hz) to the first floor along the center line of the structure, and a load cell was attached at the end of a stringer to measure the input force from the shaker to the structure. In addition, eight accelerometers were attached at the center line of each floor to measure the system's response, and the LMS-test lab system (Zhang *et al.* 2008), which had been introduced in detail in Section 4.1, was employed here to acquire the acceleration data with the sampling frequency of 512 Hz and duration time of 32s. In the study, eight different damage statuses were introduced by removing one of the three steel sheets of a column at the corresponding layer, thus a reduction in inter-layer stiffness of 8.3% was observed for each damage condition, as shown in Table 13. Thus, a total of nine test conditions were investigated, including the undamaged condition as the baseline. For each condition, the test was repeated ten times to calculate the mean values as the final measuring data.

By collecting and analyzing the measured acceleration using the LMS test Lab, the structural mode shapes and frequencies under the baseline condition were successfully obtained. On the other hand, benefit to the advantage of the proposed method during the damage identification process, only several modal frequencies of the structure under the test conditions were required and can be conveniently obtained even only one acceleration record was provided. Table 14 presents all the modal frequencies under the health (baseline) and eight damaged conditions.

## 6.2 Construction of the FCSR baseline dataset

Following the detailed procedure of the FCSR baseline construction described in Section 3.3, assuming a to-be-updated model of this eight-story frame structure under health condition existed, and its physical parameters were

all equal to one, i.e.,  $m_i = 1$ ,  $k_i = 1$  ( $i=1,2,\dots,8$ ) and  $m_1$  had been known. Thus, the other physical parameters, including the mass and stiffness matrix, of this to-be-updated model can be obtained according to the typical characteristic of the element mass-stiffness distribution of the shear building. Then, by combining with the identified modal parameters (mode shapes and frequencies) of the test structure obtained under the health condition, this assumed initial to-be-updated model can be updated using the CMCM model updating algorithm, and the updated results were presented in Table 15.

Based on this updated model, the FCSR baseline dataset of the damage location of the actual structure can be constructed by reducing the element stiffness of the updated model by 30% one by one, and then the corresponding modal frequencies for each stiffness reduction conditions can be calculated. Finally, the FCSR for each reduction scenario can be obtained by combining with the structural frequencies on health condition, as shown in Table 16, in which,  $F$  denotes the FCSR of the baseline dataset calculated based on the updated model, and  $F^*$  denotes the FCSR calculated based on actual structural physical parameters.

## 6.3 Damage localization

From the Table 14, the FCSRs of the actual structure under eight different damage conditions can be calculated by combining the frequencies obtained from the corresponding damage condition with the one obtained from the health condition. Due to the space limitation, the calculated FCSRs were not presented in detail. Then, for each damage condition, its actual FCSR will be compared with the one selected from the constructed baseline dataset for their similarity using the MAC and NMD method. The final identification result can be found in Table 17. By selecting the FCSR sample that has the maximum of MAC value and minimum of NMD value from the baseline dataset, most damaged conditions in this study were effectively identified and accurately localized. However, it should be note that although the identification for State#5 points to a wrong location, the FCSR sample with the preset damage at 4<sup>th</sup>-floor still has the second maximum of MAC (exceed 0.9) and second minimum of NMD, which presents

Table 15 The updated model using the CMCM algorithm

	Actual physical parameters	$m_1$ -normalized	The updated result	
			Initial assumption	Updated parameters
$m_1$	3.38	1	1	1
$m_2$	3.38	1	1	1
$m_3$	3.38	1	1	1
$m_4$	3.38	1	1	1
$m_5$	3.38	1	1	1
$m_6$	3.38	1	1	1
$m_7$	3.38	1	1	1
$m_8$	2.824	0.8355	1	0.8
$k_1$	$2.4129 \times 10^4$	$7.1388 \times 10^3$	1	$6.4225 \times 10^3$
$k_2$	$2.4129 \times 10^4$	$7.1388 \times 10^3$	1	$7.1825 \times 10^3$
$k_3$	$2.4129 \times 10^4$	$7.1388 \times 10^3$	1	$6.5987 \times 10^3$
$k_4$	$2.4129 \times 10^4$	$7.1388 \times 10^3$	1	$6.7567 \times 10^3$
$k_5$	$2.4129 \times 10^4$	$7.1388 \times 10^3$	1	$6.5956 \times 10^3$
$k_6$	$2.4129 \times 10^4$	$7.1388 \times 10^3$	1	$7.1473 \times 10^3$
$k_7$	$2.4129 \times 10^4$	$7.1388 \times 10^3$	1	$6.9924 \times 10^3$
$k_8$	$2.4129 \times 10^4$	$7.1388 \times 10^3$	1	$7.3585 \times 10^3$

\* all the unit of the element mass is kg, and the unit of the element stiffness is N/m

Table 16 The FCSR baseline dataset for different damage locations

		k1 (-30%)	k2 (-30%)	k3 (-30%)	k4 (-30%)	k5 (-30%)	k6 (-30%)	k7 (-30%)	k8 (-30%)
$\Delta\lambda_2/\Delta\lambda_1$	F*	7.75	4.05	0.29	2.32	13.19	31.31	55.92	78.67
	F	7.99	3.98	0.20	2.80	14.40	32.86	57.48	78.02
$\Delta\lambda_3/\Delta\lambda_1$	F*	16.17	0.66	15.94	34.46	11.43	16.52	169.63	534.54
	F	15.42	0.31	17.96	33.22	7.85	23.96	192.36	546.19
$\Delta\lambda_4/\Delta\lambda_1$	F*	20.96	8.58	47.32	0.85	76.04	57.34	119.10	1438.22
	F	18.23	10.98	47.16	0.01	85.79	36.99	160.21	1476.90
$\Delta\lambda_5/\Delta\lambda_1$	F*	20.04	54.28	15.60	81.53	9.94	193.40	0.62	2045.47
	F	16.20	61.70	12.90	98.48	1.35	241.89	7.17	2725.00
$\Delta\lambda_6/\Delta\lambda_1$	F*	14.62	70.65	21.13	40.20	146.22	24.72	391.60	1825.99
	F	12.61	77.72	21.12	36.07	153.14	68.85	267.61	2517.60
$\Delta\lambda_7/\Delta\lambda_1$	F*	7.63	42.78	90.37	47.44	2.44	176.03	521.12	1064.69
	F	8.42	54.24	96.30	67.31	6.98	97.54	547.77	1375.70
$\Delta\lambda_8/\Delta\lambda_1$	F*	2.08	12.15	31.54	70.72	128.24	141.01	166.84	308.40
	F	1.03	6.58	14.96	38.35	100.11	222.38	337.68	886.74

## 7. Conclusions

a strong correlation with the actual damaged FCSR at the correct location. This single mistake of location identification is predicted to be caused by the influence of measurement error and environmental noise, but it does not affect to draw the conclusion that the proposed FCSR-based method has the potential to realize the structural damage identification and localization, especially for the shear buildings.

The frequency-change-square-ratio (FCSR) based damage detection method can realize the damage identification and localization, even only the first several measured frequencies are provided. This distinguish advantage makes this kind method very attractive for structural health monitoring in practical applications.

Table 17 The damage location identification results using the developed method

	Floor	State#2	State#3	State#4	State#5	State#6	State#7	State#8	State#9
MAC	1	0.98	0.65	0.64	0.71	0.57	0.46	0.44	0.71
	2	0.69	0.98	0.79	0.72	0.67	0.57	0.54	0.86
	3	0.54	0.63	0.96	0.59	0.42	0.31	0.61	0.69
	4	0.75	0.76	0.66	0.92	0.38	0.69	0.60	0.83
	5	0.55	0.65	0.47	0.50	0.99	0.72	0.78	0.81
	6	0.69	0.58	0.46	0.98	0.47	0.92	0.76	0.87
	7	0.53	0.68	0.87	0.63	0.61	0.56	0.86	0.82
	8	0.86	0.87	0.71	0.86	0.72	0.71	0.62	0.92
NMD	1	0.14	0.73	0.75	0.64	0.86	1.08	1.14	0.64
	2	0.68	0.15	0.52	0.62	0.71	0.87	0.91	0.40
	3	0.92	0.76	0.20	0.84	1.18	1.51	0.80	0.68
	4	0.57	0.57	0.71	0.29	1.28	0.67	0.81	0.46
	5	0.90	0.74	1.06	1.00	0.12	0.63	0.54	0.48
	6	0.68	0.86	1.08	0.15	1.07	0.30	0.56	0.39
	7	0.94	0.69	0.39	0.76	0.80	0.89	0.40	0.47
	8	0.40	0.38	0.64	0.41	0.62	0.64	0.79	0.30

However, building a precision enough FEM model for the test structure is inevitable but difficult when applying this frequency-based method. In this paper, by combining with the cross-model cross-mode (CMCM) model updating algorithm, a novel method is developed to improve the applicability of the FCSR-based damage detection method. In this paper, according to the typical mass-stiffness distribution characteristic of shear buildings, assuming there is a to-be-updated model for this actual structure, and its element mass and stiffness were all known at the beginning. Then, this initial model was updated using the CMCM algorithm by combining with the measured modal frequencies of actual structure. Thus, the final updated model can be regarded as the representation of actual structural FEM model, because their modal parameters, including the modal frequencies and mode shapes, are almost the same. Therefore, this updated model can be employed to attend the FCSR-based damage detection procedure, and no precious FEM of the test structure is needed.

In this paper, the cross-model cross-mode (CMCM) model updating algorithm and the frequency-change-square-ratio based damage detection were briefly introduced at the beginning, and the detection procedure of the developed method was then detail summarized. In addition, the effectiveness of the developed approach was verified by a numerical simulation example of four-level shear building and two experimental investigations, including a three-story structure and an eight-story shear frame. All the results demonstrate that the developed approach has the ability to detect the presence of structural change and locate the structural section where the change occurred. The developed approach extends the application of the FCSR-based damage detection method, even only the first several structural frequencies are provided, the damage detection and localization can be realized, especially for the high noisy environment in the practical application.

## Acknowledgements

This work was partially supported by National Natural Science Foundation of China (Grant number 51708520, 51608493) and Science for Earthquake Resilience (Grant number XH19031Y). The authors would like to thank for them for their financial support.

## References

- Adeuyi, A.P. and Wu, Z. (2015), "Vibration-based damage localization in flexural structures using normalized modal macrostrain techniques from limited measurements". *Comput.-Aided Civ. Inf.*, **154**(3), 154-172.
- Allemang, R.J. (2003), "The modal assurance criterion - twenty years of use and abuse", *J. Sound Vib.*, **37**(8), 14-23.
- Cawley, P. and Adams, R.D. (1979), "The location of defects in structures from measurements of natural frequencies". *J. Strain Anal. Eng.*, **14**(2), 49-57.
- Cunha, A. and Caetano, E. (2006), "Experimental modal analysis of civil engineering structures", *J. Sound Vib.*, **40**(6), 12-20.
- Ewins, D.J. (2000), "Model validation: Correlation for updating", *Sadhana*, **25**(3), 221-234.
- Figueiredo, E., Park, G., Figueiras, J., Farrar, C. and Worden, K. (2009), "Structural health monitoring algorithm comparisons using standard data sets", No. LA-14393. Los Alamos National Laboratory (LANL), Los Alamos, NM (United States).
- Hassiotis, S. (1995), "Identification of stiffness reductions using natural frequencies", *J. Eng. Mech.-ASCE*, **121**(10), 1106-1113.
- Hearn, G. and Testa, R.B. (1991), "Modal analysis for damage detection in structures", *J. Struct. Eng.*, **117**(10), 3042-3063.
- Hu, S.L.J., Li, H. and Wang, S. (2007), "Cross-model cross-mode method for model updating", *Mech. Syst. Signal Pr.*, **21**(4), 1690-1703.
- Ismail, Z. and Ong, Z.C. (2012), "Honeycomb damage detection in a reinforced concrete beam using frequency mode shape regression". *Measurement*, **45**(5), 950-959.
- Juang, J.N. (1994), *Applied system identification*, Englewood Cliff, NJ, Prentice Hall.
- Li, B. and He, Z.J. (2011), "Frequency-based crack identification

- for static beam with rectangular cross-section”, *J. Vibroeng.*, **13**(3), 477-486.
- Liang, Y., Li, D., Song, G. and Zhan, C. (2017), “Damage detection of shear buildings through structural mass-stiffness distribution”, *Smart Struct. Syst.*, **19**(1), 11-20.
- Lieven, N.A.J. and Ewins, D.J. (1988), “Spatial correlation of mode shapes: the coordinate modal assurance criterion (COMAC)”, *Proceedings of the 6th international modal analysis conference*, **1**, 690-695.
- Liu, J.L., Wang, Z.C., Ren, W.X. and Li, X.X. (2015), “Structural time-varying damage detection using synchrosqueezing wavelet transform”, *Smart Struct. Syst.*, **15**(1), 119-133.
- Maia, N.M.M. and E Silva, J.M.M. (1997), *Theoretical and experimental modal analysis*, Research Studies Press.
- Morassi, A. and Rovere, N. (1997), “Localizing a notch in a steel frame from frequency measurements”, *J. Eng. Mech. -ASCE*, **123**(5), 422-432.
- Nagarajaiah, S. and Yang, Y. (2015), “Blind modal identification of output-only non-proportionally-damped structures by time-frequency complex independent component analysis”, *Smart Struct Syst.*, **15**(1), 81-97.
- Narkis, Y. (1994), “Identification of crack location in vibrating simply supported beams”, *J. Sound Vib.*, **172**(4), 549-558.
- Peeters, B., Lowet, G., Van der Auweraer, H. and Leuridan, J. (2004a), “A new procedure for modal parameter estimation”, *J. Sound Vib.*, **38**(1), 24-29.
- Peeters, B., Van Der Auweraer, H., Guillaume, P. and Leuridan, J. (2004b), “The PolyMAX frequency-domain method: a new standard for modal parameter estimation”, *Shock Vib.*, **11**(3-4), 395-409.
- Salawu, O. (1997), “Detection of structural damage through changes in frequency: a review”, *Eng. Struct.*, **19**(9), 718-723.
- Song, G., Cai, X., Gao, S., Suonan, J. and Li, G. (2011), “Natural frequency based protection and fault location for VSC-HVDC transmission lines”, *Adv. Power Syst. Autom. Protect. (APAP), International Conference on IEEE*, **1**, 177-182.
- Świder, J., Hetmanczyk, M. and Michalski, P. (2012), “Utilization of advanced self-diagnostic functions implemented in frequency inverters for the purpose of the computer-aided identification of operating conditions”, *J. Vibroeng.*, **14**(1), 117-122.
- Wang, J. (2009), “Study on damage detection and model updating for offshore platform structures”, Ph.D. Dissertation, Qingdao, Ocean University of China.
- Xiang, J., Chen, X. and Yang, L. (2009), “Crack identification in short shafts using wavelet-based element and neural networks”, *Struct. Eng. Mech.*, **33**(5), 543-560.
- Xiang, J., Jiang, Z., Wang, Y. and Chen, X. (2011), “Study on damage detection software of beam-like structures”, *Struct. Eng. Mech.*, **39**(1), 77-91.
- Xiang, J., Matsumoto, T., Long, J., Wang, Y. and Jiang, Z. (2012), “A simple method to detect cracks in beam-like structures”, *Smart Struct. Syst.*, **9**(4), 335-353.
- Xiang, J., Nackenhorst, Udo, Wang, Y., Jiang, Y., Gao, H., He, Y. (2014), “A new method to detect cracks in plate-like structures with through-thickness cracks”, *Smart Struct. Syst.*, **14**(3), 397-418.
- Yang, M.T. and Griffin, J.H. (1997), “A normalized modal eigenvalue approach for resolving modal interaction”, *J. Eng. Gas Turb. Power*, **119**(3), 491-499.
- Zhang, L., Jiang, F., Wang, Y. and Zhang, X. (2008), “Measurement and analysis of vibration of small agricultural machinery based on LMS Test. Lab”, *Transactions of the CSAE*, **24**(5), 100-104.